Preparation of adsorbent for phosphate recovery from aqueous solutions based on condensed tannin gel

Takeshi Ogata, Shintaro Morisada *, Yasumi Oinuma, Yoshimi Seida, Yoshio Nakano

Department of Environmental Chemistry and Engineering, Interdisciplinary Graduate School of Science and Technology, Tokyo Institute of Technology, 4259 Nagatsuta, Midori-ku, Yokohama 226-8502, Japan

ARTICLE INFO

ABSTRACT

We have synthesized an iron-loaded tannin gel as an adsorbent for phosphate recovery in aqueous solutions. The use of the tannin gel prepared from condensed tannin, which is a ubiquitous and inexpensive natural polymer, is not only cost effective and environment-friendly, but interesting because the phosphate-adsorbed gel can be expected to use directly as a fertilizer. The amount of iron loaded into the tannin gel oxidized by nitric acid was much larger than that into the non-oxidized tannin gel. This increase in the amount of the loaded iron resulted in the significant increase in the adsorption amount of phosphate onto the gel. Mössbauer spectroscopy indicated that the morphology of iron in the gel is a mono-type complex, which is formed as a result of the reaction between Fe(III) and the oxidized tannin gel with carbonyl groups. The iron-loaded tannin gel showed the adsorption selectivity for phosphate over other anions and the pH independence of phosphate adsorption in the wide range of initial pH 3–12. The phosphate adsorption isotherm for the iron-loaded tannin gel followed the Freundlich equation with constants of $K_F = 2.66$ and $1/n = 0.31$, rather than the Langmuir equation. The adsorption amount of phosphate on iron weight basis for the iron-loaded tannin gel is 31.3 mg-P/g-Fe, which indicates that iron in the gel was efficiently used for the phosphate adsorption compared with other phosphate adsorbents, such as iron hydroxides.

1. Introduction

Although phosphorus is essential for plant growth and necessary for modern agricultural techniques, the shortage of phosphate rock has become increasingly serious [1,2]. Also, phosphate has a potential to cause eutrophication in surface waters. For these reasons, it is of value to recover phosphate from environmental and waste water to overcome the resource scarcity problem as well as to avoid pollution of water environment.

A biological method [3] and a coagulation method [4] are widely utilized for the phosphate removal at industrial level [5]. Under these methods, however, it is difficult to recycle the removed phosphate. A crystallization method [6,7] could be used for the phosphate recovery, but requires complicated and precise control of the operating conditions. In contrast, an adsorption method requires the simple operating conditions and produces little sludge compared with the other methods. This indicates that the adsorption method is promising for the phosphate recovery [8].

The conventional adsorbents such as zirconia and titania are difficult to use in a practical wastewater treatment because their adsorption capacities are insufficient, and the regeneration of the used adsorbent is quite difficult in spite that these adsorbents are rather expensive. In recent years, considerable attention has been paid to the investigation of low-cost adsorbents, such as waste materials [9], by-products [10], aluminum oxide hydroxide [11], and calcined alunite [12], based on economical and environmental concerns. Iron-based compounds are remarkable as inexpensive and environment-friendly adsorbents [13–17]. Borggaard [18] reported that the phosphate adsorption capacities of the iron oxides are proportional to their specific surface areas, because phosphate is adsorbed on the hydroxy groups on their surface. In practical processes, however, the fine particles of the iron oxides with large specific surface area are difficult to handle, indicating that it is necessary to load the iron oxides into some support media to improve the handling. Recent research has thus focused on creating cheap and stable iron-loaded support media [19,20].

Tannins are one of the biomass materials that are inexpensive and ubiquitous natural polymers extracted from leaves or barks of plants and have many hydroxy groups, as shown in Fig. 1 [21]. A tannin gel, which is prepared from the tannins by cross-linking, has a significant ability to adsorb and reduce various metal ions [22–30]. Furthermore, the tannins have a potential for improving soil fertility and productivity [31–33]. Therefore, the application of the tannin gel as the support media of the iron oxides is not only
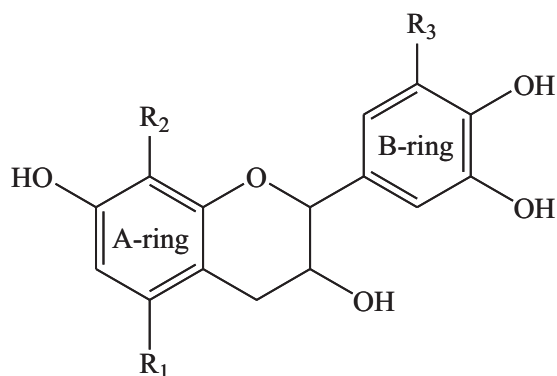
Fig. 1. Estimated chemical structure of condensed tannin molecule. (A-ring: R_1=OH, R_2=H, phloroglucinolic; R_1=R_2=H, resorcinolic; R_1=H, R_2=OH, pyrogallolic. B-ring: R_3=H, catecholic; R_3=OH, pyrogallolic) [21].

a cost effective and environment-friendly, but interesting because the phosphate-adsorbed gel can be expected to use directly as a fertilizer.

In the present study, we have developed the adsorbent for phosphate recovery utilizing the tannin gel as the support media of iron. The optimization of the iron-loaded tannin gel has been carried out in terms of the amount of iron loaded into the gel. Using the obtained iron-loaded tannin gel, the phosphate adsorption experiments have been performed at various solution conditions to investigate the effects of pH and other anionic species. Also, the adsorption isotherm has been obtained and then compared with those of other phosphate adsorbents.

2. Materials and methods

2.1. Materials

Wattle tannin powder was kindly supplied by Mitsubishi Nuclear Fuel Co., Ltd., and all other reagents were of analytical grade. The stock solutions of iron and phosphate were prepared from iron(III) nitrate nonahydrate and disodium hydrogen phosphate, respectively. Deionized and distilled water was used in all procedure, and all reagents were used as received in the present study.

2.2. Preparation of tannin gel

The tannin gel (TG) was prepared according to the previous paper [29]. Wattle tannin powder (28 g) was dissolved in 50 mL of 0.225 M sodium hydroxide solution at room temperature, and 6 mL of 37 wt% formaldehyde solution was successively added as a cross-linker. After gelation at 353 K for 12 h, the gel obtained was grinded into small particles and then washed with water and 0.05 M nitric acid solution to remove the unreacted substances, and finally rinsed with water again. The gel particles were dried by the freeze drying method.

2.3. Oxidization of tannin gel

The TG particles were oxidized using nitric acid. The TG particles (0.5 g on a dry basis) were added into 50 mL of nitric acid (1, 2, and 5 M), and then the samples were shaken in a water bath at 333 K up to 240 min. The oxidized tannin gel (OxTG) was washed with water to remove the residual nitric acid, and then dried by the freeze drying method. The attenuated total reflectance Fourier transform infrared (ATR FT-IR) spectra of the TG and the OxTG were measured by a Fourier transform infrared spectrophotometer (FT/IR 660

Plus, JASCO). To examine the optimum conditions of the oxidization treatment, the iron adsorption tests were carried out. The OxTG particles (0.05 g on a dry basis) were added into 10 mL of 0.018 mM iron(III) solution at pH 2.0, and the solution was then shaken in a water bath at 298 K for more than 5 days. The concentrations of the iron ions in the solutions were determined using an inductively coupled plasma spectrometer (ICPS) (ICPS-8100, Shimadzu), and the amounts of iron adsorbed onto the gel were calculated from the mass balance.

2.4. Preparation of iron-loaded tannin gel

The OxTG particles (2 g on a dry basis) were added into 100 mL of 1 M iron(III) solution, and the mixture was then shaken in a water bath at 298 K for more than 5 days. The iron-loaded tannin gel (FeOxTG) was separated from the solution and washed with water for a week. The gel was then filtered and freeze-dried. The iron-loaded gel using the non-oxidized TG, FeTG, was synthesized in a similar manner for comparison.

2.5. Characterization of iron-loaded tannin gel

All gels were sieved by the screens with mesh sizes of 125 and 250 μm, and the gel particles in the fraction of 125–250 μm were used in the following characterizations of the gels as well as in the phosphate adsorption experimetns. Krypton sorption measurements of the TG, the OxTG, and the FeOxTG were conducted using an Omnisorp 100CX (Beckman Coulter) at 77 K. Prior to Kr physisorption, the samples were outgassed for 1000 min at 333 K under vacuum. The specific surface areas were calculated from the Brunauer–Emmett–Teller equation over the relative pressure range $P/P_0 = 0.05 - 0.2$, where a linear relationship was maintained. Scanning electron microscope (SEM) images were obtained with a VE-7800 (Keyence) operating at an accelerating voltage in the range 1.7–2.0 kV. The electronic configuration of the FeOxTG was examined by the Mössbauer analysis. The ^{57}Fe Mössbauer spectrum for the FeOxTG was recorded at room temperature by a Mössbauer spectrometer (Topologic Systems) using ^{57}Co source (1.85 GBq).

2.6. Phosphate adsorption experiments

All phosphate adsorption experiments were carried out in a batch system. In the time-course experiments, 0.05 g (on a dry basis) of the TG, the OxTG, the FeTG, or the FeOxTG was added into 10 mL of phosphate solution (100 mg-P/L), and the mixtures were shaken in a water bath at 298 K for the specified times. In the adsorption isotherm measurements, the FeOxTG (0.05 g on a dry basis) was soaked in 10 mL of phosphate solution (10–200 mg-P/L), and the sample solutions were shaken in a water bath at 298 K for more than 5 days. To investigate the effects of pH and other anionic species on the phosphate adsorption behavior, the adsorption experiments were carried out in a manner similar to the adsorption isotherm measurements at an initial phosphate concentration of 100 mg-P/L, where initial pH and ionic strength of the solutions were adjusted using HCl, NaOH, NaCl, NaNO$_3$, and Na$_2$SO$_4$. The phosphorus concentrations of the sample solutions after filtration of the gel particles were determined by ICPS, and the amounts of phosphorus adsorbed onto the gel were calculated from the mass balance.

3. Results and discussions
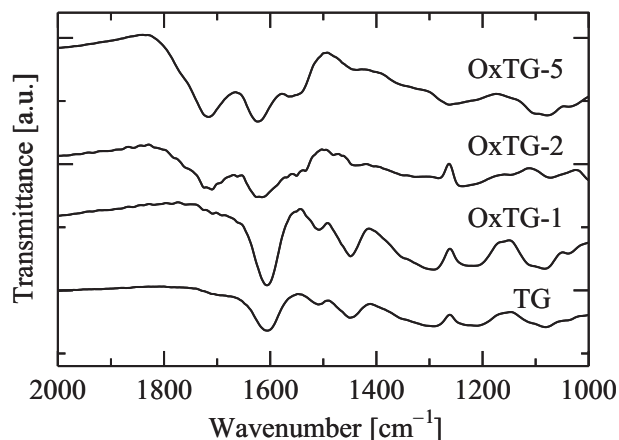
3.1. Loading of iron into tannin gel

The phosphate adsorption amount of the gel is expected to increase with an increase in the amount of iron introduced, because
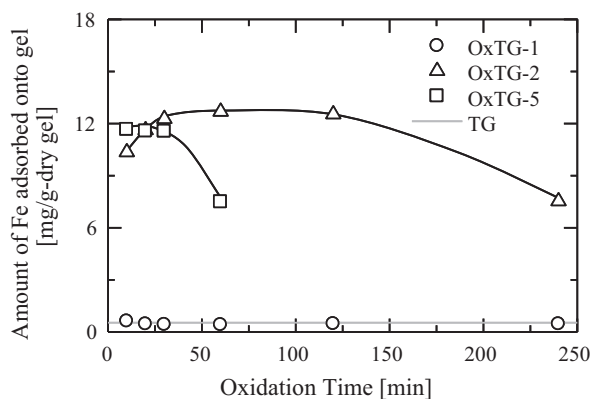
Fig. 2. Amounts of iron adsorbed onto the oxidized tannin gels (OxTGs) in 0.018 mM iron (III) solution (initial pH 2.0) at 298 K, as a function of oxidization time. The gray line represents the iron adsorption amount for the tannin gel (TG).

Table 1
Mössbauer parameters for the iron-loaded tannin gel (FeOxTG) at room temperature.

QS[a] (mm/s)	IS[b] (mm/s)	I[c] (%)	Phase
0.84	0.30	93.3	Fe(III)
2.60	0.99	6.7	Fe(II)

[a] quadrupole splitting.
[b] isomer shift.
[c] relative intensity.

the original TG does not have the ability to adsorb the phosphate ions, as will be shown in Section 3.3. To increase the iron amount in the TG, the oxidization treatment of the gel using nitric acid was carried out. The initial concentrations of nitric acid solutions used in the oxidization treatment were 1, 2, and 5 M: the gels oxidized with these concentrations of nitric acid solutions are labeled as OxTG-1, OxTG-2, and OxTG-5, respectively. The relationships between the treatment time and the amount of iron introduced into the gels are shown in Fig. 2. Under the present experimental condition, the iron ions were hardly adsorbed onto the OxTG-1 as well as the original TG, while the adsorption amounts of the iron ions for the OxTG-2 and the OxTG-5 were much larger than that for the TG.

Fig. 3 shows the ATR FT-IR spectra of the TG and the OxTGs. The spectra of the OxTG-2 and the OxTG-5, which can adsorb the iron ions as shown in Fig. 2, exhibited an absorption band at 1720–1710 cm^{-1}. This absorption band is assigned to the stretching vibration of C=O (carbonyl groups), suggesting that hydroxy groups in the gel were oxidized to carbonyl groups. Considering from the chemical structure of tannin molecule (see Fig. 1), some catecholic hydroxy groups in B-ring might be oxidized to o-benzoquinone like compounds. On the other hand, the spectrum of the OxTG-1, which showed almost no adsorption of the iron ions, exhibited no band corresponding to carbonyl groups. These results indicate that carbonyl groups formed by the oxidation of hydroxy groups play an important role in the adsorption of the iron ions. Because carbonyl groups have higher affinity to iron ions than hydroxy groups, the amounts of iron loaded into the oxidized gels were larger than that into the non-oxidized gel as seen in Fig. 2.

As shown in Fig. 2, however, the adsorption amounts of the iron ions at the long oxidization times (240 and 60 min for the OxTG-2 and the OxTG-5, respectively) were smaller than those at the shorter times, because the excessive oxidation caused the decomposition of the gel. Judging from these results, we employed the OxTG-2 oxidized for 120 min as the OxTG in all other experiments.

To prepare the FeOxTG, the iron adsorption experiment was carried out using the OxTG as shown in Fig. 4, where the TG was also used to prepare the FeTG. Note that the iron concentration in this experiment was much higher than that in the previous experiments (Fig. 2). The equilibrium values of the iron adsorption amounts for the TG and the OxTG were 36.9 and 85.1 mg-Fe/g-dry gel, respectively. Note that the amount of iron adsorbed onto the OxTG was about 2.3 times larger than that onto the TG, demonstrating that the oxidization treatment of the gel have a significant effect on the increase in the iron adsorption amount.

3.2. Characterization of iron-loaded tannin gel

The SEM images of the TG, the OxTG, and the FeOxTG were shown in Fig. 5. The pore size of the OxTG is larger than that of the TG because of the oxidization treatment, while there is hardly any difference between the OxTG and the FeOxTG. The specific surface areas obtained from the Kr sorption measurements were 0.389, 0.136, and 0.152 m^2/g for the TG, the OxTG, and the FeOxTG respectively. These results agree with the above SEM observations.

We measured the room-temperature Mössbauer spectrum of the FeOxTG to examine the morphology of iron in the gel. The resultant spectrum and parameters are shown in Fig. 6 and Table 1, respectively. The Mössbauer spectrum shows two quadrupole doublets correponding to Fe(III) and Fe(II). During the reaction of the gel and Fe(III), the formation of the complexes was accompanied by the reduction of a part of Fe(III) to Fe(II). The magnetic splitting is not observed at room temperature. Gust and Suwalski [34] measured the Mössbauer spectrum of the complex of Table 1.

Fig. 3. ATR FT-IR spectra of the tannin gel (TG) and the oxidized tannin gels (OxTGs).
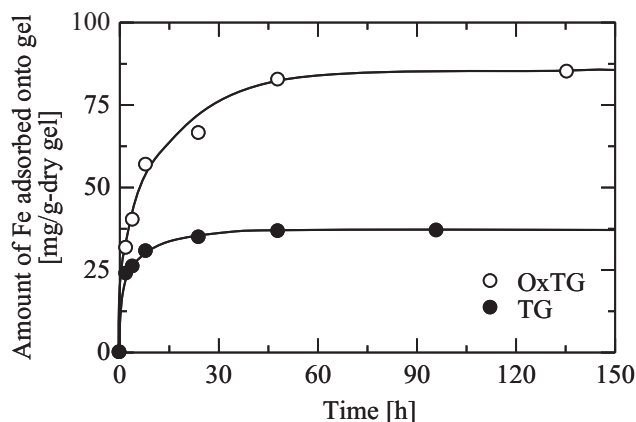
Fig. 4. Amounts of iron adsorbed onto the tannin gel (TG) and the oxidized tannin gel (OxTG) in 1 M iron(III) solution at 298 K, as a function of time.
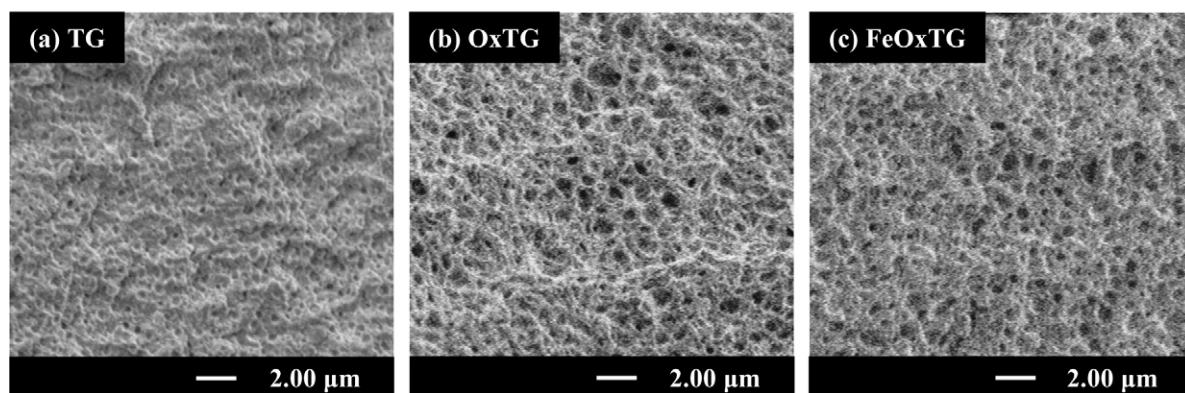
Fig. 5. SEM images of the different tannin gels: (a) the tannin gel (TG); (b) the oxidized tannin gel (OxTG); (c) the iron-loaded tannin gel (FeOxTG).

Mössbauer parameters for the iron-loaded tannin gel (FeOxTG) at room temperature.

polyphenol and the iron ions and showed the Mössbauer parameters of the mixture of mono- and bis-type complexes, which were conventionally designated as CI- and CII-types shown in Fig. 7, respectively: here, the room temperature Mössbauer parameters are quadrupole splitting (QS) = 0.80 ± 0.06 mm/s and isomer shift (IS) = 0.43 ± 0.02 mm/s for the CI-type complex, and QS = 1.19 ± 0.08 mm/s and IS = 0.44 ± 0.02 mm/s for the CII-type complex. The Mössbauer parameters for the FeOxTG listed in Table 1 fairly agree with those for the CI-type complex, indicating that most iron in the FeOxTG exists as the CI-type complex as shown in Fig. 7a.

3.3. Adsorption behavior of phosphate

The adsorption amounts of phosphate onto the gels were shown in Fig. 8, as a function of time. The TG and the OxTG, which are the non-iron-loaded gels, hardly adsorbed phosphate, indicating that the tannin itself has no ability to adsorb phosphate. In contrast, the iron-loaded gels, that is, the FeTG and the FeOxTG, can adsorb phosphate. The adsorption amount of phosphate onto the FeOxTG was much larger than that onto the FeTG because the amount of iron loaded in the former gel is larger than that in the latter one as seen in Fig. 4.

The adsorption isotherm of phosphorus onto the FeOxTG at 298 K is shown in Fig. 9. We analyzed the adsorption isotherm for the FeOxTG using the Langmuir and the Freundlich equations,
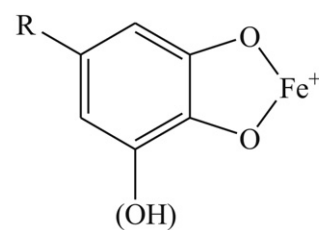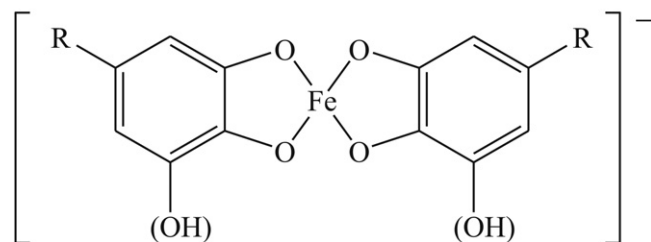
Fig. 7. Polyphenol-iron complexes: (a) CI-type; (b) CII-type. R represents the residue of the polyphenol ligand [34].
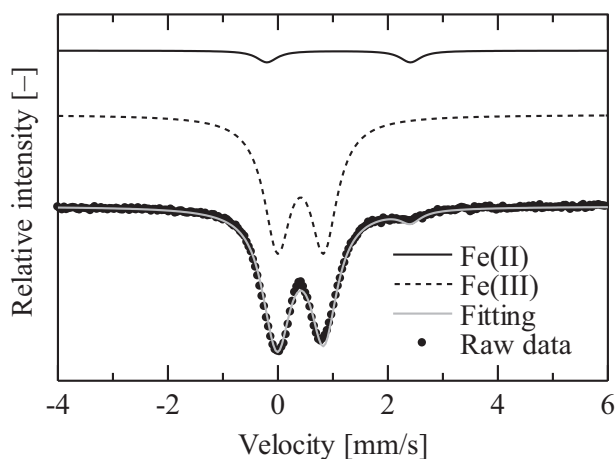

Fig. 6. Room-temperature Mössbauer spectrum of the iron-loaded tannin gel (FeOxTG). Filled symbols denote the raw data, and the lines represent the fitting results.
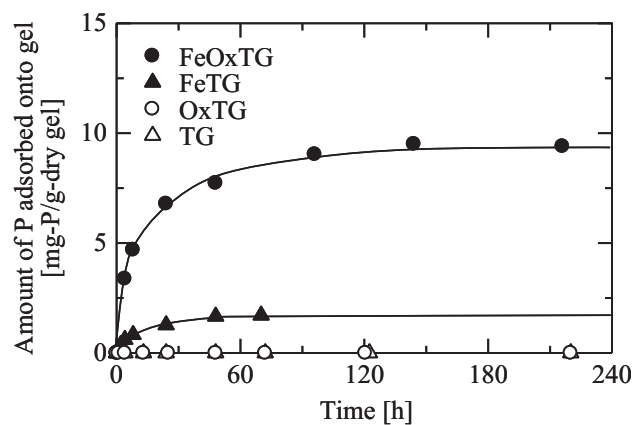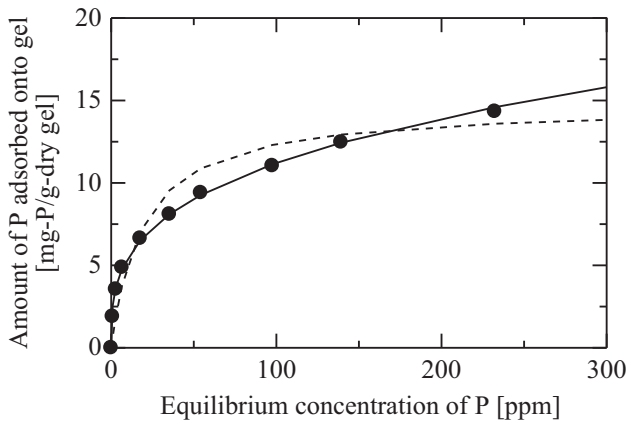

Fig. 8. Amounts of phosphorus adsorbed onto the tannin gel (TG), the oxidized tannin gel (OxTG), the iron-loaded tannin gel without oxidization (FeTG), and the iron-loaded tannin gel (FeOxTG) at 298 K, as a function of time.

Fig. 9. Adsorption isotherm of phosphorus for the iron-loaded tannin gel (FeOxTG) at 298 K. Solid and broken lines represent the Freundlich and the Langmuir isotherms.

which are commonly used to describe the adsorption isotherm. The Langmuir equation is represented by:

$$Q_e = \frac{K_L Q_m C_e}{1 + K_L C_e} \tag{1}$$

where Q_e is the equilibrium amount of phosphate adsorbed onto the gel, K_L is the Langmuir constant related to the adsorption energy, Q_m is the adsorption capacity of the gel and C_e is the equilibrium concentration of phosphorus in the solution. Eq. (1) can be rewritten in a linearized form as:

$$\frac{C_e}{Q_e} = \frac{1}{K_L Q_m} + \left(\frac{1}{Q_m}\right) C_e \tag{2}$$

We fitted Eq. (2) to the plots of C_e/Q_e against C_e and found that the values of K_L and Q_m are 0.0525 L/mg-P and 14.7 mg-P/g-dry gel, respectively. The Freundlich equation is expressed as:

$$Q_e = K_F C_e^{1/n} \tag{3}$$

where K_F and n are the Freundlich constants. These isotherm constants obtained by the linear regression were $K_F = 2.66$ and $1/n = 0.31$. The Langmuir and the Freundlich isotherms with the resultant parameters are also exhibited in Fig. 9. As is clearly seen in this figure, our experimental results of the adsorption isotherm of phosphate for the FeOxTG are faithfully represented by the Freundlich equation rather than the Langmuir equation.

To investigate the effect of initial pH (pH_{init}) on the adsorption behavior of phosphorus onto the FeOxTG, the adsorption experi-
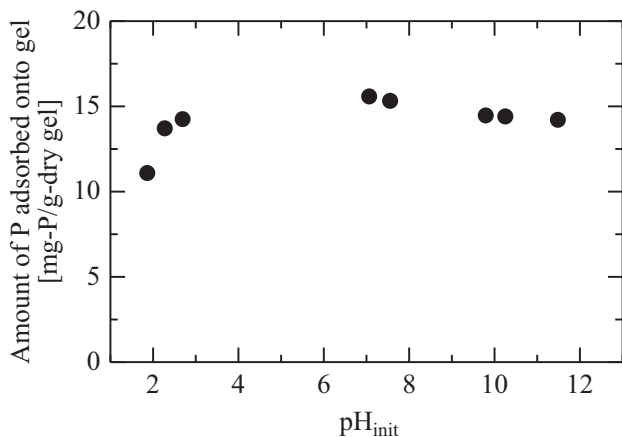
Fig. 10. Initial pH dependence of phosphorus adsorption amounts onto the iron-loaded oxidized tannin gel (FeOxTG) at ionic strength 0.1 and 298 K.
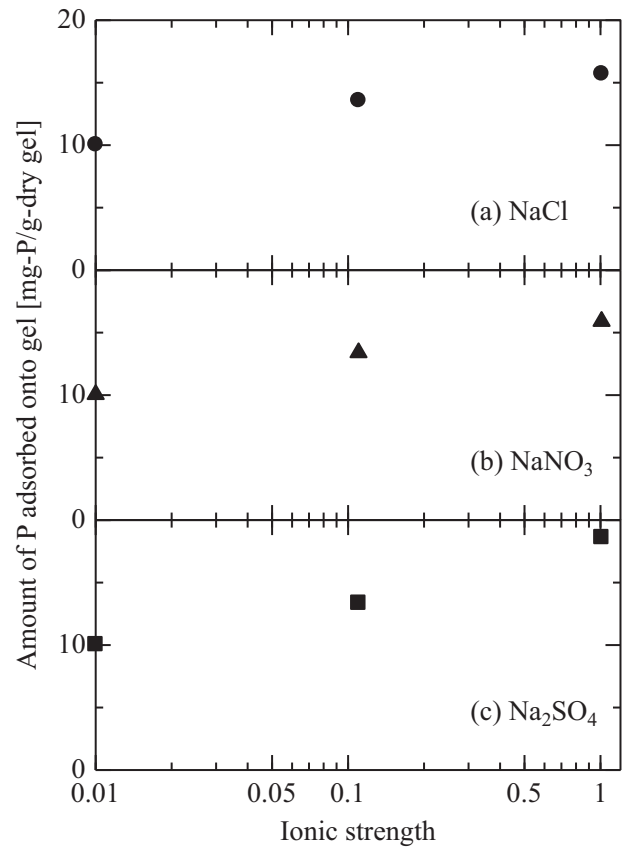
Fig. 11. Ionic strength dependence of phosphorus adsorption amounts onto and percent elution of iron from the iron-loaded oxidized tannin gel (FeOxTG) at 298 K: (a) with NaCl; (b) with NaNO$_3$; (c) with Na$_2$SO$_4$.

ments were carried out in the range of pH_{init} 2–12 at ionic strength 0.1 and 298 K: as mentioned in Section 2.6, pH_{init} and ionic strength of the solutions were adjusted using HCl, NaOH, NaCl, NaNO$_3$, and Na$_2$SO$_4$. Fig. 10 shows the amounts of phosphorus adsorbed onto the FeOxTG as a function of pH_{init}. The adsorption amount of phosphorus increased with increasing pH_{init} from 2 to 3, while in the range of pH_{init} 3–12, the adsorption amount was nearly independent of pH_{init}.

We also examined the adsorption selectivity for phosphate over other anionic species, chloride ion, nitrate ion, and sulfate ion. Fig. 11 shows the amounts of phosphorus adsorbed onto the FeOxTG at 298 K as a function of ionic strength. The adsorption amounts of phosphorus increased with increasing ionic strength of the solutions in all cases. It was worth noting that the adsorption amounts of phosphorus onto the FeOxTG increase rather than decrease with increasing concentrations of other anions. This indicates that the FeOxTG has the adsorption selectivity for phosphate ions over other anionic species.

3.4. Comparison with other phosphate adsorbents

The adsorption isotherms of phosphorus for the various iron hydroxides and the iron-based adsorbents including our FeOxTG are summarized in Table 2 [9,17,20,35]. In order to compare in lower phosphorus concentration, the amounts of phosphorus adsorbed onto each adsorbent at the phosphorus concentration of 1 mg-P/L, Q_1, are also listed. Although the value of Q_1 for the FeOxTG is reasonably good compared with other adsorbents except for Geothite and Akaganéite, which shows much larger values of Q_1. However, the weight fractions of iron in Goethite and Akaganéite are 44.1 and 52.2 wt%, respectively, while that in the FeOxTG is only

Table 2
Adsorption isotherms of phosphorus for iron hydroxides and iron-based adsorbents.

Adsorbent	Isotherm equation	Q_1[a] (mg-P/g)	Ref.
Goethite	$Q_e = 17.3C_e^{0.115}$	17.3	17
Akaganéite	$Q_e = 10.0C_e^{0.417}$	10.0	17
Iron oxide tailings	$Q_e = \dfrac{4.67C_e^{0.371}}{1+0.369C_e^{0.371}}$	3.41	9
FeOxTG	$Q_e = 2.66C_e^{0.31}$	2.66	This work
Ferromanganese nodules	$Q_e = \dfrac{3.77C_e}{1+1.55C_e}$	1.48	35
NCS[b]	$Q_e = \dfrac{0.40C_e}{1+0.23C_e}$	0.33	20
SCS[c]	$Q_e = \dfrac{0.30C_e}{1+0.20C_e}$	0.25	20
CB[d]	$Q_e = \dfrac{0.15C_e}{1+0.17C_e}$	0.13	20

[a] the amount of phosphorus adsorbed onto the adsorbent at $C_e = 1$ mg-P/L.
[b] natural iron oxide coated sand.
[c] synthetic iron oxide coated sand.
[d] iron oxide coated crushed brick.

about 8.5 wt%: that is, the phosphorus adsorption amounts on iron weight basis are 39.2, 18.1, and 31.1 mg-P/g-Fe for Goethite Akaganéite, and the FeOxTG, respectively. This indicates that iron in the FeOxTG was efficiently used for the phosphate adsorption.

4. Conclusions

We have tried to synthesize an adsorbent for phosphate recovery based on the iron-loaded tannin gel. The major conclusions are as follows:

The amount of iron introduced into the tannin gel was increased up to about 2.3 times by the oxidization treatment. This increase in the iron amount resulted in the significant increase in the adsorption amount of phosphate onto the FeOxTG.

The room-temperature Mössbauer spectrum of the FeOxTG suggested that the morphology of iron in the gel is the mono-type complex, which is formed from the reaction between Fe(III) and the OxTG with carbonyl groups.

The FeOxTG showed the adsorption selectivity for phosphate over other anions and the pH independence of phosphate adsorption in the wide range of initial pH 3–12.

The adsorption isotherm of phosphorus for the FeOxTG followed the Freundlich equation with the constants of $K_F = 2.66$ and $1/n = 0.31$. The phosphorus adsorption amount on iron weight basis for the FeOxTG bears comparison with other adsorbents.

The FeOxTG developed in the present study is promising for recovery of phosphate from environmental and waste water because this adsorbent not only is inexpensive and environment-friendly, but also can be expected to use directly used as a fertilizer.

References

[1] J.R. Herring, R.J. Fantel, Phosphate rock demand into the next century: impact on world food supply, Nat. Resour. Res. 2 (1993) 226–246.
[2] J. Driver, D. Lijmbach, I. Steen, Why recover phosphorus for recycling, and how? Environ. Technol. 20 (1999) 651–662.
[3] T. Mino, M.C.M. van Loosdrecht, J.J. Heijnen, Microbiology and biochemistry of the enhanced biological phosphate removal process, Water Res. 32 (1998) 3193–3207.
[4] S.A. Parsons, T.A. Berry, in: E. Valsami-Jones (Ed.), Phosphorus in Environmental Technologies Principles and Applications, IWA, London, 2004, pp. 260–271.
[5] G.K. Morse, S.W. Brett, J.A. Guy, J.N. Lester, Review: phosphorus removal and recovery technologies, Sci. Total Environ. 212 (1998) 69–81.
[6] J.D. Doyle, S.A. Parsons, Struvite formation, control and recovery, Water Res. 36 (2002) 3925–3940.
[7] K. Suzuki, Y. Tanaka, T. Osada, M. Waki, Removal of phosphate, magnesium and calcium from swine wastewater through crystallization enhanced by aeration, Water Res. 36 (2002) 2991–2998.
[8] K. Urano, H. Tachikawa, Process development for removal and recovery of phosphorus from wastewater by a new adsorbent. 1. Preparation method and adsorption capability of a new adsorbent, Ind. Eng. Chem. Res. 30 (1991) 1893–1896.
[9] L. Zeng, X. Li, J. Liu, Adsorptive removal of phosphate from aqueous solutions using iron oxide tailings, Water Res. 38 (2004) 1318–1326.
[10] J. Pradhan, J. Das, S. Das, R.S. Thakur, Adsorption of phosphate from aqueous solution using activated red mud, J. Colloid Interface Sci. 204 (1998) 169–172.
[11] S. Tanada, M. Kabayama, N. Kawasaki, T. Sakiyama, T. Nakamura, M. Araki, T. Tamura, Removal of phosphate by aluminum oxide hydroxide, J. Colloid Interface Sci. 257 (2003) 135–140.
[12] M. Ozacar, Equilibrium and kinetic modelling of adsorption of phosphorus on calcined alunite, Adsorption 9 (2003) 125–132.
[13] A. Ookubo, K. Ooi, H. Hayashi, Preparation and phosphate ion-exchange properties of a hydrotalcite-like compound, Langmuir 9 (1993) 1418–1422.
[14] Y. Seida, Y. Nakano, Removal of phosphate in dissolution-coagulation process of layered double hydroxide, J. Chem. Eng. Jpn. 34 (2001) 906–911.
[15] Y. Seida, Y. Nakano, Removal of phosphate by layered double hydroxides containing iron, Water Res. 36 (2002) 1306–1312.
[16] G.B. Douglas, M.S. Robb, D.N. Coad, P.W. Ford, in: E. Valsami-Jones (Ed.), Phosphorus in Environmental Technologies Principles and Applications, IWA, London, 2004, pp. 291–320.
[17] R. Chitrakar, S. Tezuka, A. Sonoda, K. Sakane, K. Ooi, T. Hirotsu, Phosphate adsorption on synthetic goethite and akaganeite, J. Colloid Interface Sci. 298 (2006) 602–608.
[18] O.K. Borggaard, Effect of surface area and mineralogy of iron oxides on their surface charge and anion-adsorption properties, Clay Clay Min. 31 (1983) 230–232.
[19] B.K. Biswas, K. Inoue, K.N. Ghimire, S. Ohta, H. Harada, K. Ohto, H. Kawakita, The adsorption of phosphate from an aquatic environment using metal-loaded orange waste, J. Colloid Interface Sci. 312 (2007) 214–223.
[20] N. Boujelben, J. Bouzid, Z. Elouear, M. Feki, F. Jamoussi, A. Montiel, Phosphorus removal from aqueous solution using iron coated natural and engineered sorbents, J. Hazard. Mater. 151 (2008) 103–110.
[21] R.W. Hemingway, J.J. Karchesy, S.J. Branham, Chemistry and Significance of Condensed Tannins, Plenum Press, New York, 1989, pp. 83–107.
[22] Y. Nakano, K. Takeshita, T. Tsutsumi, Adsorption mechanism of hexavalent chromium by redox within condensed-tannin gel, Water Res. 35 (2001) 496–500.
[23] X. Zhan, A. Miyazaki, Y. Nakano, Mechanisms of lead removal from aqueous solutions using a novel tannin gel adsorbent synthesized from natural condensed tannin, J. Chem. Eng. Jpn. 34 (2001) 1204–1210.
[24] Y.H. Kim, Y. Nakano, Adsorption mechanism of palladium by redox within condensed-tannin gel, Water Res. 39 (2005) 1324–1330.
[25] Y.H. Kim, T. Ogata, Y. Nakano, Kinetic analysis of palladium(II) adsorption process on condensed-tannin gel based on redox reaction models, Water Res. 41 (2007) 3043–3050.
[26] Y.H. Kim, Y. Ogawara, T. Ogata, Y. Nakano, Adsorption mechanism of selenite (Se⁴⁺) by redox within condensed-tannin gel under concentrated hydrochloric acid solution, Chem. Lett. 36 (2007) 1316–1317.
[27] Y.H. Kim, Y. Nakano, Effect of Br⁻ on the adsorption rate of palladium(II) ions onto condensed-tannin gel in chloride media, Sep. Sci. Technol. 43 (2008) 2386–2395.
[28] Y.H. Kim, M.N. Alam, Y. Marutani, T. Ogata, S. Morisada, Y. Nakano, Improvement of Pd(II) adsorption performance of condensed-tannin gel by amine modification, Chem. Lett. 38 (2009) 956–957.
[29] T. Ogata, Y. Nakano, Mechanisms of gold recovery from aqueous solutions using a novel tannin gel adsorbent synthesized from natural condensed tannin, Water Res. 39 (2005) 4281–4286.
[30] T. Ogata, Y.H. Kim, Y. Nakano, Selective recovery process for gold utilizing a functional gel derived from natural condensed tannin, J. Chem. Eng. Jpn. 40 (2007) 270–274.
[31] N. Fierer, J.P. Schimel, R.G. Cates, J. Zou, Influence of balsam poplar tannin fractions on carbon and nitrogen dynamics in Alaskan taiga floodplain soils, Soil Biol. Biochem. 33 (2001) 1827–1839.
[32] T.E.C. Kraus, R.A. Dahlgren, R.J. Zasoski, Tannins in nutrient dynamics of forest ecosystems—a review, Plant Soil 256 (2003) 41–66.
[33] T.E.C. Kraus, R.J. Zasoski, R.A. Dahlgren, Fertility and pH effects on polyphenol and condensed tannin concentrations in foliage and roots, Plant Soil 262 (2004) 95–109.
[34] J. Gust, J. Suwalski, Use of Mössbauer spectroscopy to study reaction products of polyphenols and iron compounds, Corrosion 50 (1994) 355–365.
[35] K.M. Parida, S. Mohanty, Studies on Indian ocean manganese nodules. VIII. Adsorption of aqueous phosphate on ferromanganese nodules, J. Colloid Interface Sci. 199 (1998) 22–27.